JOURNAL OF AGRICULTURAL AND FOOD CHEMISTRY

pubs.acs.org/JAFC Article

Warming Leads to Changes in Soil Organic Carbon Molecules Due to Decreased Mineral Protection

Li Zhang,[#] Ruilin Huang,[#] Zhiyuan Ma,[#] Sen Li, Jixian Ding, Weigen Huang, Chaoyang Liu, Yueyu Sui, Jizhong Zhou, Jiabao Zhang, and Yuting Liang[*]

Cite This: *J. Agric. Food Chem.* 2024, 72, 7765−7773 Read Online

ACCESS | Metrics & More | Article Recommendations | Supporting Information

ABSTRACT: Climate change affects the content and composition of soil organic carbon (SOC). However, warming-induced changes in the SOC compounds remain unknown. Using nuclear magnetic resonance spectroscopy, molecular mixing models, and Fourier transform ion cyclotron resonance mass spectrometry, we analyzed the variations and relationships in molecular compounds in Mollisol with 10−56 g C kg^{-1} $soil^{-1}$ by translocating soils under six climate regimes. We found that increased temperature and precipitation were negatively correlated with carbohydrate versus lipid and lignin versus protein. The former was consistent across soils with varying SOC contents, but the latter decreased as the SOC content increased. The carbohydrate−lipid correlations were related to dithionite−citrate-extractable Fe, while the lignin−protein correlations were linked to changes in moisture and pyrophosphate-extractable Fe/Al. Our findings indicate that the reduction in the mineral protection of SOC is associated with molecular alterations in SOC under warming conditions.

KEYWORDS: *soil organic carbon, extractable metals, lignin, protein, lipid, carbohydrate, climate change*

1. INTRODUCTION

Soil organic carbon (SOC) is a significant terrestrial carbon pool that surpasses both the atmosphere and oceans in terms of size.[1] SOC plays a crucial role in maintaining soil fertility and mitigating changes in the soil environment due to climate change.[2] The primary components of SOC are plant-derived compounds (e.g., lignin, carbohydrates, lipids, and proteins), microbial-derived compounds (e.g., lipids and proteins), and fire-derived carbon (also known as char, black carbon, or pyrolyzed carbon).[3] In agricultural ecosystems, microbial-derived carbon accounts for approximately 50% of the SOC composition.[4] Therefore, understanding how the molecular composition of SOC responds to changes in precipitation and temperature is essential for better predicting the impacts and feedback of soil carbon on environmental changes.[3]

The persistence of SOC is largely dependent on molecular diversity and complexity, as well as the protective role of physicochemical interactions with minerals.[3] Due to the varying responses of SOC molecular components to mineral protection and the dual role of microorganisms in decomposition and necromass contributions,[5] there are often negative correlations among soil carbon molecular compositions. SOC plays a crucial role in maintaining high crop yields and soil health in agricultural soils. Even within the same soil type under identical tillage conditions, the molecular composition of SOC can vary significantly depending on the initial organic matter content.[6] However, the changes in SOC molecules with different organic carbon contents and their responses to climate change remain unclear.

Previous studies have indicated that soils with high organic matter contents are more likely to lose organic carbon than soils with low organic matter contents under warming conditions.[7] The SOC content was significantly positively correlated with soil organic matter-associated metals such as citrate−dithionite-extractable and oxalate-extractable Fe/Al.[8] Differences in carbon loss rates in soils with high and low organic carbon may be related to the stability of the interactions between organic matter and these extractable metals.[9−11] The desorption of SOC molecules adsorbed on mineral surfaces by ligand exchange is challenging. In contrast, the desorption of SOC molecules adsorbed by cation bridging or van der Waals forces is more likely to occur.[11] Additionally, various environmental factors (e.g., precipitation, temperature, pH, and ionic strength) can affect the content of some short-range-ordered metals and the adsorption capacity of metals for SOC molecules to alter the rate of carbon loss.[12,13]

In this study, we translocated Mollisol[14] with varying initial SOC contents ranging from 10 to 56 g C kg^{-1} $soil^{-1}$ across a wide range of climatic gradients.[15] It is important to note that the different climatic regimes considered here represent integrated climate conditions where both MAT and MAP increase simultaneously. Using NMR spectroscopy, molecular mixing models, and Fourier transform ion cyclotron resonance mass spectrometry,[16] we evaluated the changes in the molecular correlations of SOC under warming conditions. We propose the following hypothesis: Different climatic regimes result in negative correlations between carbohydrate

Received: December 19, 2023
Revised: March 15, 2024
Accepted: March 19, 2024
Published: April 1, 2024

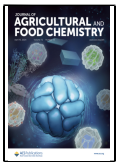

versus lipid and lignin versus protein molecules in SOC; particularly in high-carbon soils, such negative correlations are closely related to changes in soil-extractable Fe/Al levels.

2. MATERIALS AND METHODS

2.1. Site Characteristics and Experimental Design. In this study, agricultural soils with five different SOM contents were collected in 2015 in Northeast China. The SOM contents were 2, 3, 5, 7, and 9% g SOM kg^{-1} $soil^{-1}$ (equivalent to 10, 18, 28, 36, and 56 g C kg^{-1} $soil^{-1}$, respectively), and all the soils were classified as Mollisols according to the FAO classification.[14] Then, all of the soil samples were packed into the same PVC tubes and maintained in Hailun (in situ site, HL, N 47°27′, E 126°55′) and southward translocated to the other five geoclimatic locations: Shenyang (SY, N 41°49′, E 123°33′), Fengqiu (FQ, N 35°03′, E 114°23′), Changshu (CS, N 31°41′, E 120°41′), Yingtan (YT, N 28°12′, E 116°55′), and Guangzhou (GZ, N 23°23′, E 113°27′). The soil was homogenized using a 2 mm sieve and then packed into sterilized PVC tubes. The PVC tubes had a diameter of 5 cm at the bottom and a height of 31 cm. Each tube was filled with a 25 cm-high soil column corresponding to approximately 1 kg of soil. The bottom of the pipe was filled with 1 cm of quartz sand, and a 5 cm space was left at the top. The PVC pipes were buried in agricultural soil at each site to a depth of 20 cm. No plants were planted in the 2.5 m surrounding the experimental plots. From October to November 2015, 90 PVC pipes containing soil (5 SOC gradients × 3 replicates × six climatic conditions) were transported to 6 ecological research stations with different geoclimatic conditions and SOC contents, and 15 PVC pipes were placed at each site. Once the experiment was established, weeds growing in each PVC pipe were manually removed every 2−3 weeks to avoid the impact of plants. The MAT and MAP in the six locations ranged from 1.5 to 21.9 °C and from 550 to 1750 mm from north to south, respectively. The climate types at the six sites are moderate temperate continental (HL), temperate monsoon (SY), warm temperate continental monsoon (FQ), subtropical monsoon (CS), midsubtropical humid monsoon mild (YT), and maritime subtropical monsoon (GZ). The detailed experimental design can be found in Huang et al.[15]

After 1.5 years, we collected the soil samples, which were stored on dry ice and rapidly transported to the laboratory. The assayed soil variables included pH, moisture, nitrate-nitrogen (NO_3^--N), ammonium nitrogen (NH_4^+-N), total nitrogen (TN), dissolved organic carbon (DOC), microbial biomass carbon (MBC), and soil organic carbon (SOC). The microbial (e.g., bacterial and fungal) community was assessed using second-generation high-throughput sequencing technology, and the soil microbial C metabolic activity was measured with BIOLOG 96-well Eco-Microplates (Biolog Inc., USA) using 31 different carbon sources and three replicates in each microplate. All of these biochemical variables, the corresponding assays, and data can be found in our previous studies.[15]

To reveal the effect of different extractable metals (e.g., iron and aluminum) on the response of the different constituents of organic carbon (e.g., lignin, protein, carbohydrate, lipid, carbonyl, and char) to different climatic regimes, we measured different forms of aluminum (Al)-bearing minerals and iron (Fe)-bearing minerals, as well as exchangeable calcium (Ca_{Exch}). Specifically, different forms of Al-bearing minerals and Fe-bearing minerals were extracted using sodium pyrophosphate (Fe_p and Al_p), acidic ammonium oxalate (Fe_O and Al_O), and citrate-bicarbonate-dithionite (CBD) (Fe_d and Al_d) reagents.[8,17] Fe_p include organo-complexed Fe and dispersible colloidal Fe.[17] Al_p corresponds to Al in humus complexes and, in most soils, can be used to estimate Al in such complexes.[18] Fe_O often includes phases such as nanogoethite, ferrihydrite, and other short-range-ordered (SRO) phases.[18] Acidic ammonium oxalate-extractable Al (i.e., Al_O) is composed of SRO Al and organo-complexed Al in soils.[8] Fe_d includes highly crystalline [oxyhydr] oxides and SRO phases, while Al_d includes Al substituted in Fe minerals and organic complexes of Al.[8] Therefore, these extractable Fe and Al forms include oxides and organically complex and ionic forms. The exchangeable cations (CEC, i.e., H^+, K^+, Na^+, Ca^{2+}, Mg^{2+}, Al^{3+}, and Fe^{3+}) were extracted with 0.1 mol l^{-1} $BaCl_2$ (50:1, solution:soil), while the extraction of exchangeable Ca^{2+} was performed using NH_4Cl-ethanol.[19] To determine the Fe_d, Al_d, Fe_O, Al_O, Fe_p, Al_p, CEC, and Ca_{Exch} contents, all of the supernatants were analyzed by inductively coupled plasma−mass spectrometry (ICP−MS) (NexION 350x, ICP−MS Spectrometer, PerkinElmer, USA).

2.2. Solid-State ^{13}C NMR Analysis of Soil Carbon Molecular Groups. Solid-state ^{13}C nuclear magnetic resonance (NMR) spectroscopy analysis was performed to determine the molecular structure of the SOC. Before the examination, to improve the NMR sensitivity and remove the interference of paramagnetic materials in soils,[20] the samples were pretreated with hydrofluoric (HF) acid (10% v/v) to remove any calcium carbonate and mineral phases. Specifically, 5 g of air-dried soil was weighed in a 100 mL centrifuge tube with 50 mL of a hydrofluoric acid solution (10% v/v) and shaken for 1 h. The supernatant was then removed by centrifugation at 3000 r min^{-1} for 10 min. The residues were then washed with ultrasonication eight times with a hydrofluoric acid solution (10%). The oscillation program consisted of four ×1 h, three ×12 h, and one ×24 h. The soil samples were then washed with distilled water four times to remove the residual hydrofluoric acid. The treated soil samples were dried in an oven at 25 °C,[21] ground, and passed through a 60-mesh sieve for NMR measurements.

After pretreatment, the ^{13}C cross-polarization/total sideband suppression (CP-TOSS) and CP-TOSS with dipolar dephasing experiments were subjected to solid-state magic-angle spinning NMR measurements (Bruker AVANCE400, Bruker BioSpin GmbH, Karlsruhe, Germany) using 4 mm sample rotors at a ^{13}C frequency of 100 MHz, a spinning speed of 5 kHz, a CP time of 1 ms, a ^{1}H 90° pulse length of 4 μs, and a recycle delay of 0.8 s. Four-pulse TOSS was employed before detection, and two-pulse phase-modulated decoupling was applied for optimum resolution. CP-TOSS combined with 40 μs dipolar dephasing was then applied to generate a subspectrum with nonprotonated carbons and mobile groups.[22] The spectra were quantified by subdividing them into the following chemical shift regions:[23] 0−45 ppm (alkyl), 45−65 ppm (*N*-alkyl and methoxyl), 65−90 ppm (*O*-alkyl), 90−110 ppm (*di*-*O*-alkyl), 110−145 ppm (aryl), 145−165 ppm (*O*-aryl), and 165−210 ppm (carbonyl). The NMR spectra of the different sites can be found in Figure S1.

After obtaining the proportions of the seven integrated spectral regions in the sample based on the molar N:C ratios and the reported distribution of carbon in the spectral region (% of the total), we used a molecular mixing model to estimate the relative abundance of six organic carbon constituents: carbohydrate, protein, lignin, lipid, carbonyl, and char.[16] The detailed chemical structures and assignments of the organic carbon molecules can be found in Table S1.

2.3. Dissolved Organic Matter Analysis. We used Fourier transform ion cyclotron resonance mass spectrometry (FT-ICR MS) analysis to evaluate the effect of different climatic regimes on organic carbon molecules in dissolved organic matter (DOM). Solid-phase extraction (SPE-DOM) of the dissolved organic matter in the soil was performed according to the procedures described previously by Li et al.[23] Specifically, the soil DOM was first extracted with Milli-Q water (1:5 w/v) on a reciprocal shaker (170 rpm) for 8 h. The samples were then centrifuged at 2800 × g for 10 min, and the supernatant was filtered through a 0.45 μm mixed cellulose ester membrane. SPE cartridges (Bond Elut PPL, 500 mg, 6 mL, Agilent Technologies, Santa Clara, CA) were activated by sequentially rinsing with pure methanol (mass spectrometry grade) and 0.01 M HCl.[24] The acidified DOM samples (pH 2) were passed over activated cartridges. Then, the cartridges were rinsed with acidified Milli-Q water (pH 2). After the cartridges were completely dried with ultrapure N_2 gas, DOM was eluted from the cartridges with methanol (5 mL) and stored at −20 °C.

The molecular composition of the solid-phase-extractable DOM (SPE-DOM) was analyzed by using a Bruker SolariX 15.0 T FT-ICR MS instrument equipped with an electrospray ionization source (Bruker Apollo II) applied in negative mode. The injection method was continuous; the injection rate was 120 μL/h; the capillary inlet voltage was −4.0 kV; the ion accumulation time was 0.1 s; the mass

https://doi.org/10.1021/acs.jafc.3c09657
J. Agric. Food Chem. 2024, 72, 7765−7773

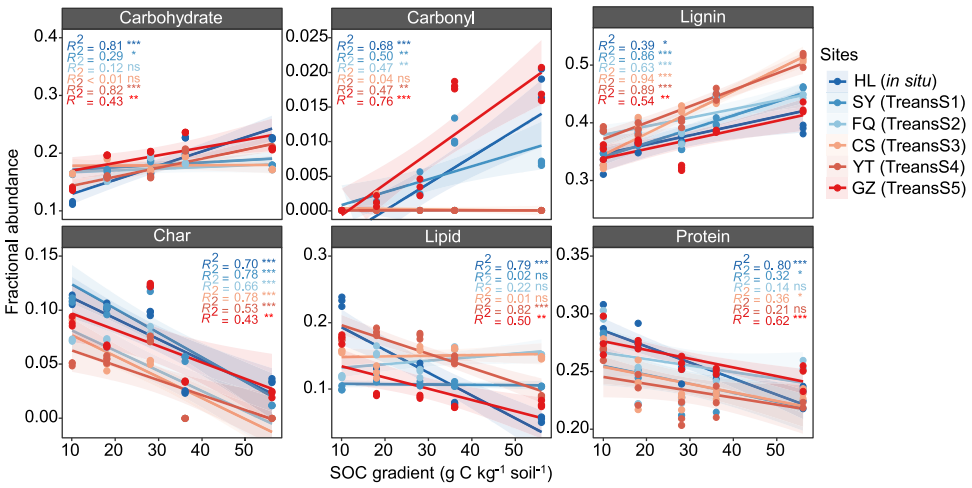

Figure 1. Regression analysis for carbon abundance as a fraction of the total SOC and initial SOC contents. Values were obtained by applying the abundance of the functional groups from ^{13}C solid-state NMR to a mixed linear model. Dots with different colors represent the observations in situ and at five translocated sites (n_{sample} = 90). Significance is indicated by $^{ns}p > 0.05$, $^{*}p < 0.05$, $^{**}p < 0.01$, and $^{***}p < 0.001$. The shaded area represents the 95% confidence interval.

range was 100−1600 Da; the number of sampling points was 4 M 32-bit data; and the time domain signal was superimposed 300 times to improve the signal-to-noise ratio. The instrument was calibrated with 10 mmol/L sodium formate before sample detection, and internal standard calibration was performed with soluble organic matter (known molecular formula) after sample detection. After calibration, the mass errors of the assays were less than one ppm. In the following data processing step, only detected mass peaks with a signal-to-noise ratio greater than 4 were included.[25] Molecular formula assignment was performed using Bruker Data analysis (version 4.2) with no restriction on the number of C, H, or O in the molecular formula assignment and a maximum of three N elements and one sulfur element in the molecular formula.[26] The molecules were classified as carboxyl-rich alicyclic molecules (CRAMs), where DBE/C was between 0.30 and 0.68, DBE/H was between 0.20 and 0.95, and DBE/O was between 0.77 and 1.75, according to Hertkorn et al.[27] A modified aromaticity index (AI_{mod}) was calculated for individual molecular formulas per the methods published by Koch et al.[28] Formulas with $1.5 \leq H/C \leq 2.0$, $O/C \leq 0.9$, and $N = 0$ were defined as lipids.[29] Formulas with $O/C > 0.9$ were defined as carbohydrates, while proteins with $O/C \leq 1.5 \leq H/C \leq 2.0$ and $N > 0$[30] were defined as proteins. Formulas with $0.1 < O/C < 0.6$, $0.6 < H/C < 1.7$, and $AI_{mod} < 0.67$ were classified as lignin.[31]

2.4. Statistical Analysis. The relative abundance of the six organic carbon constituents in the soils with different initial SOC contents was analyzed using R (version 4.1.2) (https://www.r-project.org/). Rotated principal component analysis (RPCA)[8] was used to assess the relationships among the relative abundances of the four major SOC molecules calculated from the molecular mixing models[16] and soil biogeochemical variables. Using molecular mixing models, we evaluated the relative abundances of different organic carbon molecules; R scripts can be found in the Supporting Information. The principal components (PCs) were calculated from the correlation matrix of the carbon molecule data and rotated orthogonally (varimax rotation) using the "psych" package (version 2.1.9)[32] in R version 4.1.2. Rotation is commonly used in principal component analysis (PCA) to simplify PC interpretation by maximizing/minimizing the correlation between the factor and the component axes.[33] These rotated components (RCs) of the correlation matrix were used to facilitate the interpretation of each component according to the significant carbon molecules.[8] We calculated the correlations between the two RCs (i.e., RC1 and RC2) and the four main carbon molecules, the correlations between the two RCs and all of the detected biogeochemical variables, and the correlations between the four organic carbon molecules and all of the biogeochemical variables using the rcorr function in the "Hmisc" (version 4.6-0) package.[34]

The importance and explanatory effects of the models composed of biogeochemical variables in terms of the changes in the four organic carbon molecules and the RC axis were assessed using the random forest algorithm.[35] In the course of the random forest model's operations, the explanatory effects of the models were analyzed using the randomForest function, the explanatory effects and significance of the model were assessed using the rf.significance function with a 999 permutation test, and the significance and importance of each biogeochemical variable were assessed using the rfPermute function with a 999 permutation test. The R packages included "randomForest" (version 4.6-14),[35] "rfUtilities" (version 2.1-5),[36] and "rfPermute" (version 2.5).[37] Additionally, to investigate the relationships among the different biogeochemical variables, we used linear fit analysis. PCA was employed to obtain the PC axis with the highest explained amount for the nutrient content-related matrix.[38] The results showed that the PC1 axis explained 65% of the nutrient content-related matrix and was significantly correlated with all of the detected nutrient factors. ($r < -0.80$, $p < 0.001$; Figure S2). Consequently, we chose the product of the −1 and PC1 axes as a proxy for the nutrient content in the soil.

Structural equation models (SEMs) were fitted to illustrate the direct or indirect effects of different climatic regimes (e.g., MAT and MAP), soil properties (e.g., pH and moisture), soil carbon metabolic activity, and extractable metals on each RC (representing the negative correlations among organic carbon molecules).[39] Axis 1 of the PCA was used to represent all extractable metals to reduce the number of variables in the SEMs. The prior model was constructed based on the literature review and our analyses. For example, random forest analysis indicated that extractable metals, pH, moisture content, microbial metabolic activity, and climatic regime (MAP and MAT) were consistently of significant importance for the negative correlation between carbohydrates and lipids (represented by RC1) and between lignin and protein (represented by RC2) (Figure S3); hence, these variables were selected for constructing the SEMs in this study. We performed logarithmic transformation for the variables that did not conform to a normal distribution and used the χ^2 test (the model was assumed to exhibit a good fit if $p > 0.05$), the goodness-of-fit index (GFI; the model was assumed to show a good fit if GFI > 0.9), the root-mean-square error of approximation (RMSEA; the model was assumed to exhibit a good fit if RMSEA < 0.05 and $p > 0.05$),[40] and the Bollen−Stine bootstrap test (the model was assumed to show a good fit if the bootstrap $p > 0.10$) to test the overall goodness of fit of the SEM. All SEM analyses were conducted using IBM SPSS Amos 21.0 (AMOS, IBM, USA).

https://doi.org/10.1021/acs.jafc.3c09657
J. Agric. Food Chem. 2024, 72, 7765−7773

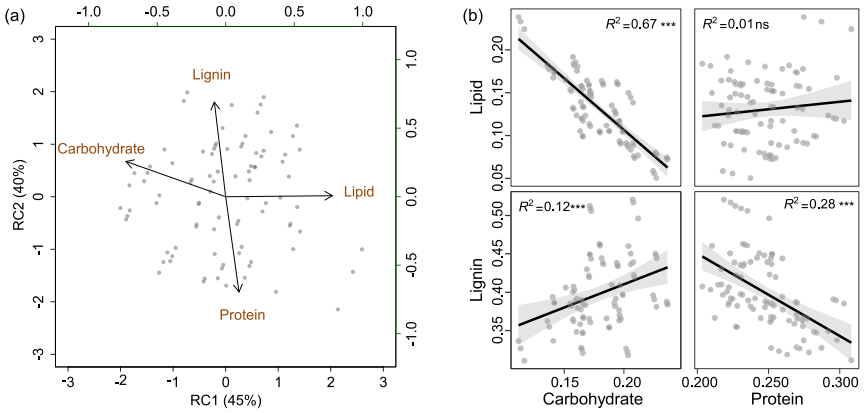

Figure 2. RPCA of SOC molecules in all samples (a) and regression analysis for different SOC molecules (b). Gray dots represent soil samples (n_{sample} = 90). Labeled arrows in the RPCA plot indicate correlations between SOC molecules and RCs. Lines in the regression plot represent linear regressions, and colored shading represents 95% confidence intervals. Significance is indicated by $^{ns}p > 0.05$, $*p < 0.05$, $**p < 0.01$, and $***p < 0.001$. The raw data are provided in the open data repository figshare.

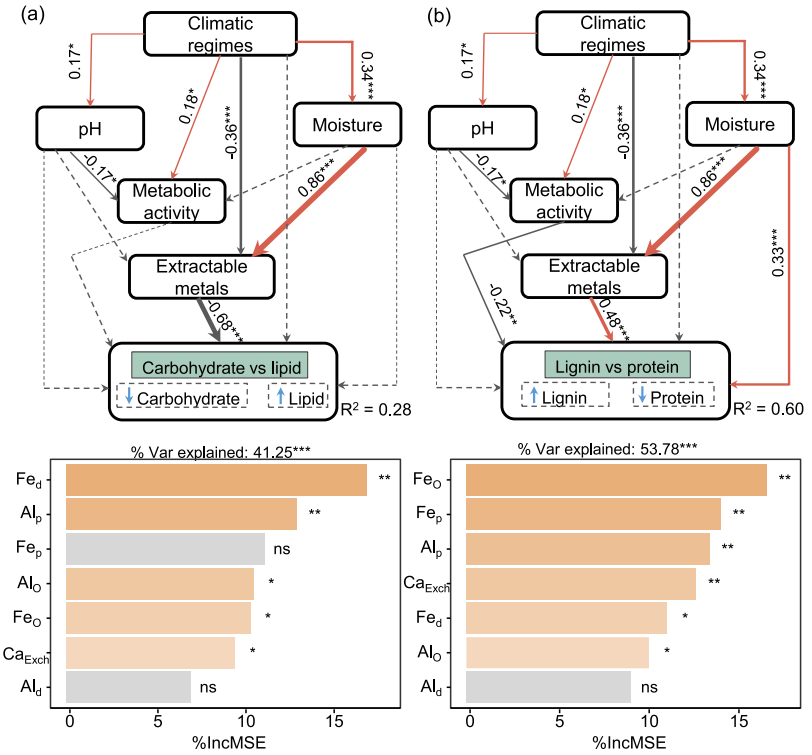

Figure 3. SEMs and random forest models of the SOC molecular composition. The response variables for carbohydrate vs lipid and lignin vs protein are represented by the RC1 and RC2 axes in Figure 2. The upward (↓) and downward (↑) arrows indicate positive and negative correlations, respectively, between C molecules and the rotation axis. (a) $\chi^2/df = 0.27$, $p = 0.76$; GFI = 0.98, AGFI = 0.95; RMSEA= 0.00, $p = 0.80$; bootstrap $p = 0.75$. (b), $\chi^2/df = 0.27$, $p = 0.76$; GFI = 0.99, AGFI = 0.98; RMSEA = 0.00, $p = 0.80$; bootstrap $p = 0.76$. The solid red line with arrows, the solid gray line with arrows, and the dashed gray line with arrows represent significant positive, significant negative, and nonsignificant correlations, respectively. The numbers adjacent to the arrows are the correlation coefficients. R^2 is the model's amount of interpretation for the response variable. Significance is indicated by $^{ns}p > 0.05$, $*p < 0.05$, $**p < 0.01$, and $***p < 0.001$.

3. RESULTS

3.1. Molecular Variations in SOC in Soils. The SOC composition in the soils (10, 18, 28, 36, and 56 g C kg^{-1} $soil^{-1}$) was determined by ^{13}C NMR spectroscopy analysis (Figure S4a). The main functional groups in the SOC were alkyl, O-alkyl, and aryl C, and their relative proportions were related to the SOC content. For example, alkyl C decreased (from 32.15 to 17.01% on average) as the SOC increased (10–56 g kg^{-1}), whereas *O*-alkyl C increased (from 14.80 to 24.00% on average) as the SOC increased. Using a molecular mixing model, we further assessed the relative abundance of microbial-, plant-, and fire-derived carbon (Figure S4b). Lignin (39.85%) and protein (24.79%) were the two dominant constituent molecules, followed by carbohydrate (18.02%) and lipid (13.04%), while char (5.66%) and carbonyl (0.28%) accounted for only a small part of the SOC. A quantitative comparison of the effects of initial SOC content and different climatic regimes on the molecular changes in the six constituents using permutational multivariate analysis of variance revealed that initial SOC content (R^2 = 0.53, *F*

https://doi.org/10.1021/acs.jafc.3c09657
J. Agric. Food Chem. 2024, 72, 7765−7773

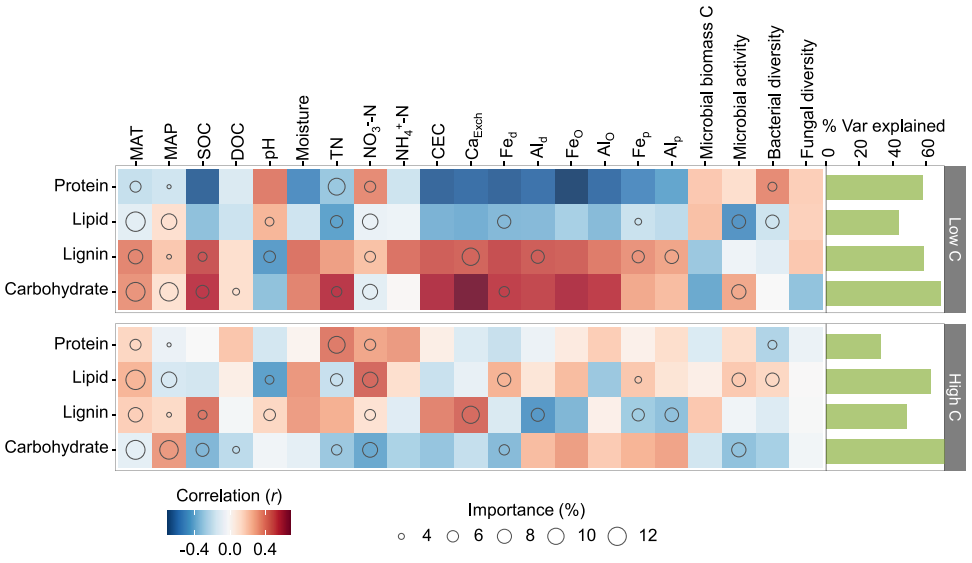

Figure 4. Contribution of biogeochemical variables to four molecular abundance changes based on correlation analysis and random forest models in low-C and high-C soils. The colors illustrate Pearson's correlations. Blue represents a negative correlation, and red represents a positive correlation. The circle size represents the importance of the variables in the random forest model, in which only the significantly ($p < 0.05$) important circles are displayed. In the bar plot, the height of the bars represents the amount of biogeochemical variables explained by changes in the abundance of constituent molecules.

value = 393, $p < 0.001$) was more closely related to the relative abundance of carbon molecules than was the climatic regime ($R^2 = 0.21$, F value = 124, $p < 0.001$, Table S2).

3.2. Different Climatic Regimes Induced Negative Molecular Correlations of SOC. Because lignin, carbohydrates, proteins, and lipids accounted for approximately 96% of the total SOC (Figures 1 and S4), we focused our analysis on these four constituent molecules. We found that although the organic carbon composition varied greatly between samples with different initial organic carbon contents, the molecules covaried predictably in samples with the same initial SOC content. Under different climatic regimes, significant negative correlations were observed between carbohydrates and lipids ($r_{mean} = -0.874$, $p < 0.001$) and between lignin and protein ($r_{mean} = -0.76$, $p < 0.001$) in soils with 10−56 g C kg^{-1} $soil^{-1}$ (Figure S5).

RPCA revealed that the correlation matrix of the SOC molecules was primarily explained by two axes (Figures 2a and S5a). In all of the samples ($n = 90$), the two RCs explained 85% of the SOC molecule correlation matrix (Figure 2a). Rotation axis 1 (i.e., RC1) explained 45% of the SOC molecule correlation matrix, while rotation axis 2 (i.e., RC2) explained 40%. The SOC molecule correlation matrix explained by the two RCs in the soils with five SOC gradients was 78, 89, 90, 82, and 89%, respectively (Figure S6a). Furthermore, correlation analysis between the two RCs and the different organic carbon molecules revealed that there was a consistent and significant correlation ($p < 0.001$) between the same RC (RC1 or RC2) and carbohydrate and/or lipid (Figure S6b), and the correlation coefficient values between the two C molecules (carbohydrate and lipid) and RCs were consistently opposite ($r_{carbohydrate} = 0.95$, 0.99, 0.84, 0.75, and −0.87; $r_{lipid} = -0.98$, −0.79, −0.90, −0.65, and 0.90). Similarly, significant correlations were found between the same RC and lignin and/or protein in samples with organic carbon contents of 10 and 18 g C kg^{-1} $soil^{-1}$, with opposite correlation coefficients ($r_{lignin} = -0.85$ and −0.95; $r_{protein} = 0.51$ and 0.81).

3.3. Relationships between SOC Molecular Changes and Climatic and Edaphic Variables. The relationships between the relative abundance of SOC molecules and climatic and soil edaphic variables were analyzed. The results revealed that in all samples ($n = 90$), the four SOC molecules (carbohydrates, lignin, lipids, and proteins) exhibited significant correlations with most geochemical, climatic, and biological variables ($p < 0.05$) (Figure S7). Considering that pairwise correlations are only applicable for revealing linear relationships between factors, we implemented a random forest model (Figure S7). The results showed that in all samples, the model composed of all biogeochemical factors explained 77.24, 76.17, 60.63, and 67.98% of the changes in the carbohydrate, lignin, lipid, and protein contents, respectively ($p < 0.001$). The most significant variables affecting these contents were Ca_{Exch}, SOC, Fe_d, and Fe_O (importance = 13.30, 14.87, 13.25, and 14.16%, respectively). Other essential predictors included MAT, MAP, DOC, TN, Ca_{Exch}, and Al_p.

To further assess the direct and indirect effects of different climatic regimes (i.e., MAP and MAT) and the effects of pH, moisture, microbial metabolic activity, and extractable metals (i.e., Ca_{Exch}, Fe_d, Al_d, Fe_O, Al_O, Fe_p, and Al_p) on the two major negative correlations, that is, carbohydrate versus lipid and lignin versus protein, we constructed SEMs (Figure 3). For the carbohydrate versus lipid negative correlations, different climatic regimes decreased the relative abundance of carbohydrates and increased the relative abundance of lipids directly and indirectly (e.g., by increasing moisture), affecting the extractable metal content (e.g., $Fe_{d\ importance}$ = 17.1% and $Al_{p\ importance}$ = 13.1%, Figure 3a). Similarly, different climatic regimes directly or indirectly increased the relative abundance of protein and decreased the relative abundance of lignin by affecting the extractable metal content (e.g., Fe_O, Fe_p, and Al_p, Figure 3b). The standard total effect analysis showed that extractable metals were most closely correlated with carbohydrate−lipid negative correlations (Figure S8). In contrast, moisture was the factor most closely tied to the negative

https://doi.org/10.1021/acs.jafc.3c09657
J. Agric. Food Chem. 2024, 72, 7765−7773

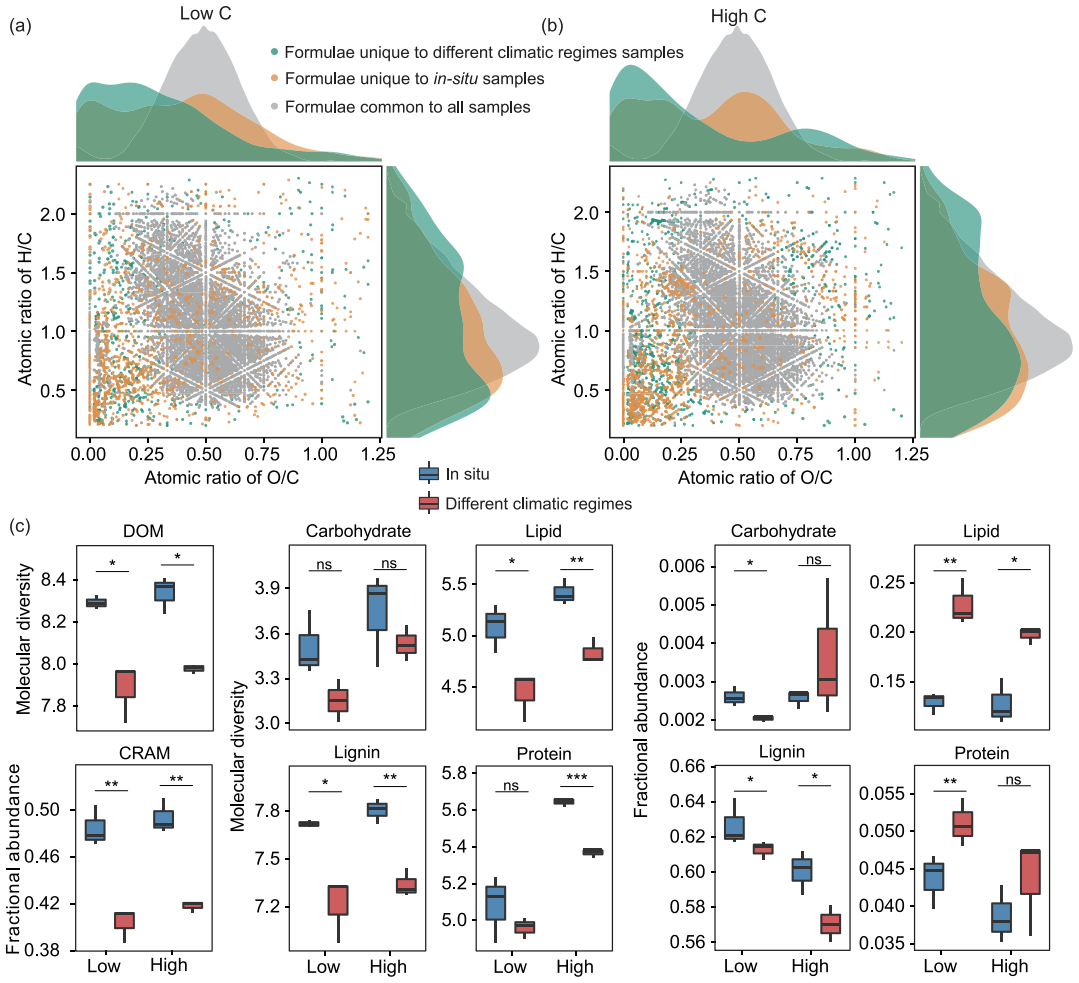

Figure 5. Effect of different climatic regimes on the dissolved organic matter (DOM). In low- (a) and high-C (b) soils, van Krevelen diagram (VKD) with marginal density plots of molecular formulas. The VKD shows formulas unique to different climatic regimes (green), in situ (orange), and molecular formulas common to all samples (gray). (c) Effects of different climatic regimes on the diversity and relative abundance of overall DOM and other DOM components.

correlations between lignin and protein, followed by extractable metals such as Fe_O, Fe_p, and Al_p.

3.4. Changes in Extractable Metals under Different Climatic Regimes. Our results showed a significant increase in exchangeable calcium (Ca_{Exch}) and extractable Fe/Al with increasing initial SOC content ($p < 0.001$, Figure S9). However, the effects of MAT and MAP on Ca_{Exch}, Fe_d, Al_d, Fe_O, Al_O, Fe_p, and Al_p were not consistent in soils with the same initial SOC content (Figure S10). For example, MAT and MAP were significantly ($p < 0.05$) positively correlated with Ca_{Exch} but negatively correlated with Fe_d and Al_d as well as Fe_p and Al_p. Moreover, the absolute values of the fitted slopes of the MAT and MAP with Ca_{Exch}, Fe_p, and Al_p clearly increased with the initial SOC content (Figure S10).

Our findings showed that a significant negative correlation existed between lignin and protein in soils with organic carbon contents below 28 g C kg^{-1} $soil^{-1}$ (Figure S5). In contrast, no significant relationship was detected in soils with organic carbon contents exceeding 28 g of C kg^{-1} $soil^{-1}$. Mollisols are a type of soil rich in SOC. Typically, Mollisols with SOC content below 32 g C kg^{-1} $soil^{-1}$ are classified as low in carbon.[41] For the purpose of our study, to enhance clarity in analysis and conclusions, we have categorized soils with an initial SOC content of less than 28 g C kg^{-1} $soil^{-1}$ as low-C soils and those with an initial SOC content exceeding 28 g C kg^{-1} $soil^{-1}$ as high-C soils. The two RCs (RC1 and RC2) explained 87 and 80% of the SOC molecular correlation matrix in the low- and high-C samples, respectively (Figure S11). The correlation and random forest analyses showed that the amount of variation in the carbohydrate, lignin, lipid, and protein contents was explained differently by the models composed of all biogeochemical factors, especially lipids and proteins (Figure 4). The correlations of extractable metals (i.e., Ca_{Exch}, Fe_d, Al_d, Fe_O, Al_O, Fe_p, and Al_p) with different organic carbon molecules were distinctly lower in high-C soils than in low-C soils. In contrast, the correlations among microbial activity, bacterial diversity, and organic carbon molecules increased.

3.5. Effects of Different Climatic Regimes on DOM Composition. Our results showed that 79,693 molecular formulas were putatively assigned (the average of all samples was 6641) in all of the soil samples (Figure S12). A total of 82.35% (5469 molecules) of all of the molecular formulas were shared among all of the tested soil samples (Figures 5a,b and S13). The van Krevelen diagram (VKD) showed that these shared molecular formulas were primarily clustered in the middle O/C and middle H/C regions. In contrast, the unique molecular formulas were mainly clustered in the low O/C and/or high-o/c regions in the low- and high-C samples. Diversity

https://doi.org/10.1021/acs.jafc.3c09657
J. Agric. Food Chem. 2024, 72, 7765−7773

analysis revealed that different climatic regimes significantly ($p < 0.05$) reduced the overall molecular diversity of the DOM, lipids and lignin (Figure 5c). In addition, different climatic regimes reduced the relative abundance of carboxylic-rich alicyclic molecules (CRAM), carbohydrates, and lignin while increasing the relative abundance of lipids and proteins.

4. DISCUSSION

Mollisol soils are fertile soils rich in SOC that can maintain high crop yields and support agricultural production. Understanding the relationships among SOC molecules and their responses to temperature and precipitation changes is highly important for protecting soils in a changing world. In all soils, two groups with negative correlations for the SOC constituent molecules were identified under different climatic regimes: lignin versus protein and carbohydrate versus lipid (Figure 2b). On average, these groups explained 83.5% of the variation in the organic carbon composition, which means that there may be a fixed compensation mechanism between the different components of the SOC.[18] In terms of the SOC composition, the negative correlations between lignin and protein and between carbohydrate and lipid may be influenced by the relationships between soil-extractable metals (e.g., Fe/Al) and SOC molecules.[9] Soil-extractable metals selectively adsorb SOC molecules.[42] Studies have shown that soil Fe/Al preferentially adsorbs lignin rather than aliphatic carbon[42] because most lignin is hydrophobic and rich in aromatic functional groups. These negatively charged functional groups interact with lignin molecules through the electrostatic adsorption of metal cations or through ligand exchange with hydroxyl groups on metal oxide surfaces to produce stable organometallic complexes.[43] Similarly, carbohydrates containing abundant carboxyl or alcohol hydroxyl groups can also form organometallic complexes with metal oxides.[10] Here, we also observed a positive correlation between dithionite−citrate-extractable Al (Al_d), acid−oxalate-extractable Fe/Al (Fe_O/Al_O), and pyrophosphate-extractable Fe/Al (Fe_p/Al_p) and lignin and carbohydrate contents (Figure 4), indicating their potential close relationships. The selectivity of these extractable metals for the adsorption of different organic carbon molecules may be one of the reasons for the negative carbohydrate versus lipid correlations and negative lignin versus protein correlations under different climatic regimes.

In this study, we further found that the negative correlations between carbohydrates and lipids did not differ among soils with different initial organic carbon contents, while the negative correlations between lignin and protein were significantly weaker in soils with high initial organic matter contents (36 and 56 g kg^{-1}) than in soils with low initial organic carbon contents (10 and 18 g kg^{-1}) (Figure S6). For the former (carbohydrates versus lipids), extractable metals such as dithionite−citrate-extractable Fe (Fe_d)) were the primary factors influencing the negative correlations (Figures 3 and S7). For the latter, moisture changes were the dominant factor influencing the negative correlations (Figure S8), followed by Fe_O, Fe_p, and Al_p (Figure 3). Previous studies have shown that Fe_d consists largely of crystalline Fe and short-range-ordered Fe[8]. Our results showed that Fe_d decreases significantly with MAT and MAP ($p < 0.05$, Figure S10), implying that the Fe_d extracted in this study may represent primarily metals in the short-range-ordered phase, as it is unlikely that crystalline Fe will undergo changes in the short term.[44] Subsequent analyses revealed no apparent differences in the response (i.e., fitting slope) of Fe_d to MAT and MAP in soils with different initial organic carbon contents (Figure S10). This may be one reason why the carbohydrate-to-lipid negative correlations did not differ between soils with different initial organic carbon contents.

In contrast, we found a significant increase in moisture content with increasing initial organic carbon content (Figure S14), which was expected to alter the negative lignin-to-protein correlations. First, a high moisture content could reduce the diffusion limitation of microbes,[45] which is expected to increase the decomposition of organic carbon by microbes under different climatic regimes.[15] Second, since soils with high organic carbon content have high water retention,[46] they are likely to show a greater risk of water logging under different climatic regimes, resulting in greater oxygen limitation than in soils with low initial organic carbon content. Studies have shown that waterlogging and oxygen limitation-induced reducing conditions and an increase in iron-reducing bacteria promote mineral dissolution[47] and enhance the bioavailability of organic carbon.[48] Under different climatic regimes, this would lead to increased organic carbon loss in soils with high initial organic carbon contents (Figures S15 and S16) and may be one of the reasons for the varied sensitivity of Fe_p and Al_p to hydrothermal changes in soils with different initial organic carbon contents (Figure S10).

In addition, our previous studies have suggested that the slower bacterial community turnover in high-C soils than in low-C soils will reduce the contribution of bacterial residues to the SOC.[5,15] Conversely, a greater turnover rate of fungal communities in high-C soils than in low-C soils will increase the contribution of fungal residues to the SOC.[5,15] Microbial biomass C is mainly derived from fungal residues rather than bacterial residues,[4] and the microbial community turnover rate correlates with the C decomposition rate of microbes.[49] Thus, under distinct climatic regimes, differences in the bacterial and fungal community turnover rates in low- and high-C soils may alter the trade-off between lignin and protein.

In summary, we used various analytical techniques to investigate the changes in molecular compounds in Mollisol soils under different climate conditions. We found that increased temperature and precipitation led to two negative correlations in SOC composition: carbohydrate versus lipid and lignin versus protein. The carbohydrate−lipid correlation was related to Fe, while the lignin−protein correlation was linked to moisture and Fe/Al. It should be noted that our results were obtained by observing only Mollisols. Ultisols distributed in warm regions generally have greater microbial transformation activity than Mollisols distributed mainly in cold regions.[50] Further work is needed to investigate the role of mineral protection in the SOC component transformation in different soil types. These findings highlight the importance of mineral protection to the molecular structure of SOC in changing climates.

■ ASSOCIATED CONTENT

Data Availability Statement

The raw sequence data for the 16S rRNA and ITS gene amplicons were deposited in the Sequence Read Archive (SRA) at the NCBI under accession no. PRJNA689098 and in the Genome Sequence Archive in the BIG Data Center, Beijing Institute of Genomics (BIG), Chinese Academy of Sciences (http://bigd.big.ac.cn/gsa), under accession no. CRA003750. Other data sets used and analyzed during the current study are

https://doi.org/10.1021/acs.jafc.3c09657
J. Agric. Food Chem. 2024, 72, 7765−7773

available from the corresponding author upon reasonable request.

Supporting Information

The Supporting Information is available free of charge at https://pubs.acs.org/doi/10.1021/acs.jafc.3c09657.

Additional experimental details, figures, and tables, including NMR spectra for all compounds (PDF)

AUTHOR INFORMATION

Corresponding Author

Yuting Liang − *State Key Laboratory of Soil and Sustainable Agriculture, Institute of Soil Science, Chinese Academy of Sciences, Nanjing 210008, China; University of Chinese Academy of Sciences, Beijing 100049, China;* orcid.org/0000-0001-5443-4486; Email: ytliang@issas.ac.cn

Authors

Li Zhang − *State Key Laboratory of Soil and Sustainable Agriculture, Institute of Soil Science, Chinese Academy of Sciences, Nanjing 210008, China; University of Chinese Academy of Sciences, Beijing 100049, China*

Ruilin Huang − *College of Resource and Environment, Anhui Science and Technology University, Chuzhou 233100, China*

Zhiyuan Ma − *State Key Laboratory of Soil and Sustainable Agriculture, Institute of Soil Science, Chinese Academy of Sciences, Nanjing 210008, China*

Sen Li − *State Key Laboratory of Soil and Sustainable Agriculture, Institute of Soil Science, Chinese Academy of Sciences, Nanjing 210008, China*

Jixian Ding − *State Key Laboratory of Soil and Sustainable Agriculture, Institute of Soil Science, Chinese Academy of Sciences, Nanjing 210008, China*

Weigen Huang − *State Key Laboratory of Soil and Sustainable Agriculture, Institute of Soil Science, Chinese Academy of Sciences, Nanjing 210008, China; University of Chinese Academy of Sciences, Beijing 100049, China*

Chaoyang Liu − *State Key Laboratory of Soil and Sustainable Agriculture, Institute of Soil Science, Chinese Academy of Sciences, Nanjing 210008, China; University of Chinese Academy of Sciences, Beijing 100049, China*

Yueyu Sui − *Northeast Institute of Geography and Agricultural Ecology, Chinese Academy of Sciences, Harbin 150040, China*

Jizhong Zhou − *School of Biological Sciences, University of Oklahoma, Norman, Oklahoma 73069, United States*

Jiabao Zhang − *State Key Laboratory of Soil and Sustainable Agriculture, Institute of Soil Science, Chinese Academy of Sciences, Nanjing 210008, China;* orcid.org/0000-0001-6922-0480

Complete contact information is available at: https://pubs.acs.org/10.1021/acs.jafc.3c09657

Author Contributions

#L.Z., R.H., and Z.M. contributed equally.

Notes

The authors declare no competing financial interest.

ACKNOWLEDGMENTS

The authors are grateful to the Editor and anonymous reviewers. We would like to thank Dr. Yimin Chen for his help with the experimental setup and sampling. This study was supported by the National Natural Science Foundation of China (42377121), the Natural Science Foundation of Jiangsu Province (BK20210994), the Jiangsu Funding Program for Excellent Postdoctoral Talent (2022ZB467), the Innovation Program of Institute of Soil Science (ISSASIP2201), and the Youth Innovation Promotion Association of the Chinese Academy of Sciences.

REFERENCES

(1) Houghton, R. A. Balancing the Global Carbon Budget. *Annual Review of Earth and Planetary Sciences.* **2007**, *35* (1), 313−347.

(2) Lal, R. Soil Carbon Sequestration Impacts on Global Climate Change and Food Security. *Science.* **2004**, *304* (5677), 1623−1627.

(3) Hall, S. J.; Ye, C.; Weintraub, S. R.; Hockaday, W. C. Molecular trade-offs in soil organic carbon composition at continental scale. *Nature Geoscience.* **2020**, *13* (10), 687−692.

(4) Liang, C.; Amelung, W.; Lehmann, J.; Kästner, M. Quantitative assessment of microbial necromass contribution to soil organic matter. *Global Change Biology.* **2019**, *25* (11), 3578−3590.

(5) Liang, C.; Zhu, X. The soil Microbial Carbon Pump as a new concept for terrestrial carbon sequestration. *Science China Earth Sciences.* **2021**, *64* (4), 545−558.

(6) Audette, Y.; Congreves, K. A.; Schneider, K.; Zaro, G. C.; Nunes, A. L. P.; Zhang, H.; Voroney, R. P. The effect of agroecosystem management on the distribution of C functional groups in soil organic matter: A review. *Biology and Fertility of Soils.* **2021**, *57* (7), 881−894.

(7) Crowther, T. W.; Todd-Brown, K. E. O.; Rowe, C. W.; Wieder, W. R.; Carey, J. C.; Machmuller, M. B.; Snoek, B. L.; Fang, S.; Zhou, G.; Allison, S. D.; Blair, J. M.; Bridgham, S. D.; Burton, A. J.; Carrillo, Y.; Reich, P. B.; Clark, J. S.; Classen, A. T.; Dijkstra, F. A.; Elberling, B.; Emmett, B. A.; Estiarte, M.; Frey, S. D.; Guo, J.; Harte, J.; Jiang, L.; Johnson, B. R.; Kröel-Dulay, G.; Larsen, K. S.; Laudon, H.; Lavallee, J. M.; Luo, Y.; Lupascu, M.; Ma, L. N.; Marhan, S.; Michelsen, A.; Mohan, J.; Niu, S.; Pendall, E.; Peñuelas, J.; Pfeifer-Meister, L.; Poll, C.; Reinsch, S.; Reynolds, L. L.; Schmidt, I. K.; Sistla, S.; Sokol, N. W.; Templer, P. H.; Treseder, K. K.; Welker, J. M.; Bradford, M. A. Quantifying global soil carbon losses in response to warming. *Nature.* **2016**, *540* (7631), 104−108.

(8) Hall, S. J.; Thompson, A. What do relationships between extractable metals and soil organic carbon concentrations mean? *Soil Science Society of America Journal.* **2022**, *86* (2), 195−208.

(9) Angst, G.; Mueller, K. E.; Nierop, K. G. J.; Simpson, M. J. Plant- or microbial-derived? A review on the molecular composition of stabilized soil organic matter. *Soil Biology and Biochemistry.* **2021**, *156*, No. 108189.

(10) Bao, Y.; Bolan, N. S.; Lai, J.; Wang, Y.; Jin, X.; Kirkham, M. B.; Wu, X.; Fang, Z.; Zhang, Y.; Wang, H. Interactions between organic matter and Fe (hydr)oxides and their influences on immobilization and remobilization of metal(loid)s: A review. *Critical Reviews in Environmental Science and Technology.* **2022**, *52* (22), 4016−4037.

(11) Mikutta, R.; Mikutta, C.; Kalbitz, K.; Scheel, T.; Kaiser, K.; Jahn, R. Biodegradation of forest floor organic matter bound to minerals via different binding mechanisms. *Geochim. Cosmochim. Acta* **2007**, *71* (10), 2569−2590.

(12) Bäckström, M.; Dario, M.; Karlsson, S.; Allard, B. Effects of a fulvic acid on the adsorption of mercury and cadmium on goethite. *Science of The Total Environment.* **2003**, *304* (1), 257−268.

(13) Islam, M. A.; Morton, D. W.; Johnson, B. B.; Angove, M. J. Adsorption of humic and fulvic acids onto a range of adsorbents in aqueous systems, and their effect on the adsorption of other species: A review. *Separation and Purification Technology.* **2020**, *247*, No. 116949.

(14) Chesworth, W.; Arbestain, M.; Macías, F.; Spaargaren, O.; Spaargaren, O.; Mualem, Y.; Eytoux, H. J. M.; Horwath, W.; Almendros, G.; Chesworth, W. *Classification of Soils: World Reference Base (WRB) for Soil Resources.* In Encyclopedia of Soil Science. Encyclopedia of Earth Sciences Series. Springer: Dordrecht, 2016, DOI: DOI: 10.1007/978-1-4020-3995-9_104.

(15) Huang, R.; Crowther, T. W.; Sui, Y.; Sun, B.; Liang, Y. High stability and metabolic capacity of bacterial community promote the rapid reduction of easily decomposing carbon in soil. *Communications Biology.* **2021**, *4*, 1.
(16) Baldock, J. A.; Masiello, C. A.; Gélinas, Y.; Hedges, J. I. Cycling and composition of organic matter in terrestrial and marine ecosystems. *Marine Chemistry.* **2004**, *92* (1−4), 39−64.
(17) Parfitt, R. L.; Childs, C. W. Estimation of forms of Fe and Al; a review, and analysis of contrasting soils by dissolution and Moessbauer methods. *Australian journal of soil research.* **1988**, *26* (1), 121−144.
(18) Hall, S. J.; Berhe, A. A.; Thompson, A. Order from disorder: do soil organic matter composition and turnover co-vary with iron phase crystallinity? *Biogeochemistry.* **2018**, *140* (1), 93−110.
(19) Gruba, P.; Mulder, J. Tree species affect cation exchange capacity (CEC) and cation binding properties of organic matter in acid forest soils. *Science of The Total Environment.* **2015**, *511*, 655−662.
(20) Mao, J. D.; Hu, W. G.; Schmidt-Rohr, K.; Davies, G.; Ghabbour, E. A.; Xing, B. Quantitative characterization of humic substances by solid-state carbon-13 nuclear magnetic resonance. *Soil Science Society of America journal.* **2000**, *64* (3), 873−884.
(21) Mathers, N. J.; Xu, Z.; Berners-Price, S. J.; Senake Perera, M. C.; Saffigna, P. G. Hydrofluoric acid pre-treatment for improving 13C CPMAS NMR spectral quality of forest soils in south-east Queensland, Australia. *Soil Research.* **2002**, *40* (4), 665.
(22) Dixon, W. T. Spinning-sideband-free and spinning-sideband-only NMR spectra in spinning samples. *Journal of Chemical Physics.* **1982**, *77* (4), 1800−1809.
(23) Li, X.; Chen, Q.; He, C.; Shi, Q.; Chen, S.; Reid, B. J.; Zhu, Y.; Sun, G. Organic Carbon Amendments Affect the Chemodiversity of Soil Dissolved Organic Matter and Its Associations with Soil Microbial Communities. *Environmental Science & Technology.* **2019**, *53* (1), 50−59.
(24) Lv, J.; Zhang, S.; Wang, S.; Luo, L.; Cao, D.; Christie, P. Molecular-Scale Investigation with ESI-FT-ICR-MS on Fractionation of Dissolved Organic Matter Induced by Adsorption on Iron Oxyhydroxides. *Environ. Sci. Technol.* **2016**, *50* (5), 2328−2336.
(25) Kujawinski, E. B.; Longnecker, K.; Blough, N. V.; Vecchio, R. D.; Finlay, L.; Kitner, J. B.; Giovannoni, S. J. Identification of possible source markers in marine dissolved organic matter using ultrahigh resolution mass spectrometry. *Geochim. Cosmochim. Acta* **2009**, *73* (15), 4384−4399.
(26) Fu, Q.; Fujii, M.; Riedel, T. Development and comparison of formula assignment algorithms for ultrahigh-resolution mass spectra of natural organic matter. *Anal. Chim. Acta* **2020**, *1125*, 247−257.
(27) Hertkorn, N.; Benner, R.; Frommberger, M.; Schmitt-Kopplin, P.; Witt, M.; Kaiser, K.; Kettrup, A.; Hedges, J. I. Characterization of a major refractory component of marine dissolved organic matter. *Geochim. Cosmochim. Acta* **2006**, *70* (12), 2990−3010.
(28) Koch, B. P.; Dittmar, T. From mass to structure: an aromaticity index for high-resolution mass data of natural organic matter. *Rapid Commun. Mass Spectrom.* **2006**, *20* (5), 926−932.
(29) McDonough, L. K.; Andersen, M. S.; Behnke, M. I.; Rutlidge, H.; Oudone, P.; Meredith, K.; O Carroll, D. M.; Santos, I. R.; Marjo, C. E.; Spencer, R. G. M.; McKenna, A. M.; Baker, A. A new conceptual framework for the transformation of groundwater dissolved organic matter. *Nat. Commun.* **2022**, *13* (1), No. 2153.
(30) Kellerman, A. M.; Dittmar, T.; Kothawala, D. N.; Tranvik, L. J. Chemodiversity of dissolved organic matter in lakes driven by climate and hydrology. *Nature Communications.* **2014**, *5*, 1.
(31) Patriarca, C.; Bergquist, J.; Sjöberg, P. J. R.; Tranvik, L.; Hawkes, J. A. Online HPLC-ESI-HRMS Method for the Analysis and Comparison of Different Dissolved Organic Matter Samples. *Environmental Science & Technology.* **2018**, *52* (4), 2091−2099.
(32) Revelle, W. *psych: Procedures for Psychological, Psychometric, and Personality Research*. Northwestern University: Evanston, Illinois, USA, 2021.
(33) Legendre, P.; Gallagher, E. D. Ecologically meaningful transformations for ordination of species data. *Oecologia.* **2001**, *129* (2), 271−280.
(34) Harrell, Jr, F. E. *Hmisc: Harrell Miscellaneous. R package version 4.7−0*. 2022.
(35) Liaw, A.; Wiener, M.Classification and Regression by randomForest. *R News* **2002**, *23*, 23.
(36) Evans, J. S.; Cushman, S. A. Gradient modeling of conifer species using random forests. *Landscape Ecology.* **2009**, *24* (5), 673−683.
(37) Archer, E. *rfPermute: Estimate Permutation p-Values for Random Forest Importance Metrics*; R Package Version 2.5, 2021
(38) Qin, S.; Kou, D.; Mao, C.; Chen, Y.; Chen, L.; Yang, Y. Temperature sensitivity of permafrost carbon release mediated by mineral and microbial properties. *Science. Advances.* **2021**, *7* (32), No. eabe3596.
(39) Grace, J. *Structural Equation Modeling and Natural Systems*. Fish & Fisheries, **2006**.
(40) Schermelleh-Engel, K.; Moosbrugger, H.; Müller, H. Evaluating the Fit of Structural Equation Models: Tests of Significance and Descriptive Goodness-of-Fit Measures. *MPR Online* **2003**, *8* (8), 23−74.
(41) Chen, X.; You, M. Y.; H, X. Z.; Lu, X. H.; Zou, W. X.; Yan, J. Native soil organic-carbon contents shape distinct bacterial communities associated with priming effect. *Pedobiologia* **2022**, *95*, No. 150842.
(42) Chassé, A. W.; Ohno, T. Higher Molecular Mass Organic Matter Molecules Compete with Orthophosphate for Adsorption to Iron (Oxy)hydroxide. *Environmental Science & Technology.* **2016**, *50* (14), 7461−7469.
(43) Chekli, L.; Phuntsho, S.; Roy, M.; Shon, H. K. Characterisation of Fe-oxide nanoparticles coated with humic acid and Suwannee River natural organic matter. *Science of The Total Environment.* **2013**, *461−462*, 19−27.
(44) Colombo, C.; Palumbo, G.; He, J.; Pinton, R.; Cesco, S. Review on iron availability in soil: interaction of Fe minerals, plants, and microbes. *Journal of Soils and Sediments.* **2014**, *14* (3), 538−548.
(45) de Vries, F. T.; Shade, A. Controls on soil microbial community stability under climate change. *Frontiers in Microbiology.* **2013**, *4*, 4.
(46) Rawls, W. J.; Pachepsky, Y. A.; Ritchie, J. C.; Sobecki, T. M.; Bloodworth, H. Effect of soil organic carbon on soil water retention. *Geoderma.* **2003**, *116* (1−2), 61−76.
(47) Patzner, M. S.; Mueller, C. W.; Malusova, M.; Baur, M.; Nikeleit, V.; Scholten, T.; Hoeschen, C.; Byrne, J. M.; Borch, T.; Kappler, A.; Bryce, C. Iron mineral dissolution releases iron and associated organic carbon during permafrost thaw. *Nature Communications.* **2020**, *11*, 1.
(48) Huang, W.; Hall, S. J. Elevated moisture stimulates carbon loss from mineral soils by releasing protected organic matter. *Nature Communications.* **2017**, *8*, 1.
(49) Glassman, S. I.; Weihe, C.; Li, J.; Albright, M. B. N.; Looby, C. I.; Martiny, A. C.; Treseder, K. K.; Allison, S. D.; Martiny, J. B. H. Decomposition responses to climate depend on microbial community composition. *Proc. Natl. Acad. Sci. U. S. A.* **2018**, *115* (47), 11994−11999.
(50) Huang, W. G.; Kuzyakov, Y.; Niu, S. L.; Luo, Y.; Sun, B.; Zhang, J. B.; Liang, Y. T. Drivers of microbially and plant-derived carbon in topsoil and subsoil. *Global Change Biol.* **2023**, *29* (22), 6188.

https://doi.org/10.1021/acs.jafc.3c09657
J. Agric. Food Chem. 2024, 72, 7765−7773